AD-A114 525 WASHINGTON UNIV SEATTLE DEPT OF MECHANICAL ENGINEERING F/G 20/11
DYNAMIC CRACK BRANCHING - A PHOTOELASTIC EVALUATION,(U)
MAY 82 M RAMULU, A S KOBAYASHI, B S KANG N00014-76-C-0060
UNCLASSIFIED UWA/DME/TR-82/43 NL

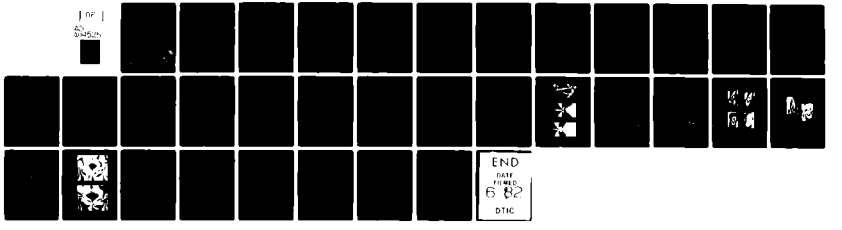

Office of Naval Research

Contract N00014-76-C-0060 NR 064-478

Technical Report No. UWA/DME/TR-82/43

DYNAMIC CRACK BRANCHING - A PHOTOELASTIC EVALUATION

by

M. Ramulu, A. S. Kobayashi and B.S.-J. Kang

May 1982

The research reported in this technical report was made possible through support extended to the Department of Mechanical Engineering, University of Washington, by the Office of Naval Research under Contract N00014-76-C-0060 NR 064-478. Reproduction in whole or in part is permitted for any purpose of the United States Government.

Department of Mechanical Engineering
College of Engineering
University of Washington

Dynamic Crack Branching - A Photoelastic Evaluation

by

M. Ramulu, A. S. Kobayashi and B. S.-J. Kang

Department of Mechanical Engineering
College of Engineering
University of Washington
Seattle, WA 98195

ABSTRACT

A necessary and sufficient condition for crack branching based on a crack branching stress intensity factor, K_{Ib}, accompanied by a minimum characteristic distance of r_c is proposed. This crack branching criterion is evaluated by dynamic photoelastic experiments involving crack branching of six single-edged notch specimens and six wedge-loaded rectangular double cantilever beam specimens. Consistent crack branching at K_{Ib} = 2.04 MPa$\sqrt{m}$ and r_c = 1.3 mm verified this crack branching criterion. The crack branching angle predicted by this crack branching criterion agreed well with those measured in the crack branching experiments.

INTRODUCTION

Literature on crack branching criteria can be grouped into two categories of dynamic crack tip stress field distortion [1,2,3]* and initiation of the secondary cracks [4-7]. While the former relates only to the singular stress field at the crack tip, the latter incorporates the nonsingular stress components. Studies on the crack tip stress field can also be divided into pre- and post-branching analyses. Pre-branching analysis normally leads to a branching criterion, while direction of the branched crack and its propagation are studied in post-branching analysis. An excellent review of such crack branching analysis can be found in Reference [7].

Crack branching has been frequently observed during the ten plus years of dynamic fracture research at the University of Washington [8] and at the University of Maryland [9]. Earlier attempts to evaluate these crack branching results were hampered by the lack of adequate data reduction procedure as well as by the paucity of theoretical understanding on elastodynamic crack propagation. Much of these obstacles have removed today and thus, it appears apropos to re-evaluate these photoelastic data on crack branching in view of the available new data reduction procedure [10]. This data analysis will be preceded by a brief review of existing crack branching criteria, after which a new crack branching criterion will be presented.

---

*Numbers in bracket refer to references at the end of this paper.

BRIEF REVIEW OF CRACK BRANCHING CRITERIA

The most popularly held cause of dynamic crack branching is the pre-branching distortion of the crack tip stress field at a critical crack velocity. Yoffe's theoretical analysis [1] of a constant velocity crack showed that at a crack velocity of about $c/c_1 = 0.33$*, the maximum circumferential stress, $\sigma_{\theta\theta}$**, shifted away from its original location of $\theta = 0$ at a lower crack velocity. This crack branching criterion based on dynamic crack kinking was followed by that of Craggs [11], who derived a critical crack velocity of $c/c_1 = 0.40$ for a propagating semi-infinite crack. Unfortunately, experimentally measured crack velocities never attained the high velocity predicted by this critical crack velocity criterion. Although Döll measured a branching crack velocity of $c/c_1 \approx 0.28$ and 0.3 in glass, [12], but the crack branching velocities in steels reported by Irwin [6], Hahn et al. [13], Congleton et al. [5], and in photoelastic polymers reported by A. S. Kobayashi et al. [8], and by T. Kobayashi and Dally [14] were less than $c/c_1 = 0.25$. Also, the precise ultrasonic ripple marking techniques used to mark instantaneous crack front by Kerkhoff [15] showed only a ten percent decrease in crack speed in glass immediately after branching, while Schardin [16] observed no change in crack velocity in plate glass. Acloque [17] observed only a six percent decrease in crack velocities immediately after branching in prestressed glass. Thus, the experimentally observed lower branching velocities, which hardly decreased after crack branching, showed that the postulated critical crack velocity could not be a prerequisite to crack branching in these materials.

---

*c and c_1 are crack velocity and dilatational stress wave velocity, respectively.

**In terms of polar coordinate (r,θ) with origin at the crack tip.

Since crack branching is also observed at extremely low crack velocity, such as that in stress corrosion cracking, other crack tip parameters such as the stress intensity factor, which could trigger branching of a crack propagating at any crack velocity must be sought. For example, attempts have been made to determine experimentally a critical crack branching stress intensity factor, K_{Ib}. Kobayashi et al. [8] showed that crack branching occurred in Homalite-100 single edge notch (SEN) specimens when K_I reached a maximum value of 3.6 times its fracture toughness, K_{IC}. Dally et al. [9,14] obtained a $K_{Ib} = 3.8\ K_{IC}$ from SEN, double cantilever beam (DCB) and compact specimens when the cracks are propagating at terminal velocity in Homalite100.

A crack kinking criterion, which is based on the development of secondary cracks in a region off-axis to the primary crack, is also an attractive alternate since the crack kinking angle is governed by the dynamic crack tip state of stress. Historically, Clark and Irwin [18] concluded that branching occurs by advanced off-axis cracking under critical stress intensity factor, K_{Ib} at a limiting crack velocity which was smaller than those of Yoffe and Craggs. These advanced cracks created crack surface of increasing roughness which were associated with increasing stress and velocity and which usually terminated after crack branching.

CRACK BRANCHING ANGLE

A characteristic feature of a branched crack is the crack branching angle and many attempts have been made to predict this crack branching. Sih [19] used the pre-branching minimum strain energy density to predict a branching angle of 15-18 degrees which varies with Poisson's ratio. Kitagawa [20] and Kalthoff [21] used the static post branching state of stress

of a symmetrically branched edged cracks and postulated that the small initial wedge angle between two branched crack was governed by a vanishing mode II stress intensity factor, i.e., $K_{II} = 0$. Kitagawa et al. predicted a branching angle of 30-40 degrees while Kalthoff's predicted branching angle of 28 degrees agreed with his measured angle in fracturing glass.

The branching angles measured by Christie [22] in an SEN specimen impacted by stress waves was about 25 degrees, while Congleton [5] observed branching angles of about 30-40 degrees in center and edge-notched steel plates and 70-80 degrees in bursting steel tubes. It will be shown later that this variation in measured crack branching angles can be attributed to the influence of a non-singular stress terms which govern the direction of crack branching in various fracture specimen geometry.

CRACK BRANCHING CRITERION

As described above, experimental evidences indicate that dynamic crack branching at a terminal crack velocity is accompanied by a critical dynamic stress intensity factor and that the crack branching angles associated with each specimen configuration are very similar. A plausible crack branching criterion would be to postulate that the crack branching stress intensity factor, K_{Ib}, as a necessary condition accompanied by a sufficient condition for crack kinking which governs the crack branching angle. The former necessary condition is supported by the crack branching data which shows that K_{Ib} is about four times its fracture toughness in Homalite-100.

As for the latter sufficient condition, either of the two dynamic crack curving criteria [23] advanced by the authors can be used to estimate the crack branching angle. These dynamic crack kinking criteria are derived from the near field, mixed mode elasto-dynamic state of stress

associated with a crack tip propagating at constant velocity. The dynamic state of crack tip stress field is given by Freund [24] in terms of local rectangular and polar coordinates of (x,y) and (r,θ), respectively, and the mode I and II dynamic stress intensity factors, K_I and K_{II}*, respectively. The second order term of σ_{ox}, which is acting parallel to the direction of crack extension, is also included in the above crack tip state of stress so that crack kinking can be triggered at crack velocities lower than those of Yoffe [1] and Craggs [11]. The two crack kinking criteria based on this dynamic crack tip stress are the maximum circumferential stress and the minimum strain energy density criteria, both of which will predict nearly identical crack kinking angles in the crack velocity range of $c/c_1 < 0.2$. Thus for brevity, only the crack kinking criterion based on the maximum circumferential stress criterion will be discussed in this paper.

The angle, θ_c, at which circumferential stress, $\sigma_{\theta\theta}$, is maximum, when evaluated in conjunction with a pure mode I dynamic crack tip state of stress will yield a transcendental relation between the critical values of θ and r as

$$r = \frac{1}{4\pi}\left[\left(\frac{K_I}{\sigma_{ox}}\right)\frac{B_1(c)}{\sin 2\theta}\left\{\left((S_1^2-S_2^2)-(1+S_1^2)\cos 2\theta\right)\frac{\partial f_{11}}{\partial\theta}\right.\right.$$
$$+\ 2(1+S_1^2)\sin 2\theta\, f_{11} + \frac{4S_1S_2}{1+S_2^2}\cos 2\theta\,\frac{\partial f_{22}}{\partial\theta}$$
$$-2\frac{4S_1S_2}{1+S_2^2}\sin 2\theta\, f_{22} - (2S_1\sin 2\theta)\left(\frac{\partial g_{11}}{\partial\theta}-\frac{\partial g_{22}}{\partial\theta}\right)$$
$$\left.\left.-(4S_1\cos 2\theta)(g_{11}-g_{22})\right\}\right]^2 \qquad (1a)$$

*The superscript "dyn" to identify dynamic stress intensity factor will not be used in this paper, since all quantities refer to dynamic values.

where

$$\left.\begin{aligned} f_{11} &= [f(c_1) + g(c_1)]^{1/2} \\ g_{11} &= [f(c_1) - g(c_1)]^{1/2} \\ f_{22} &= [f(c_2) + g(c_2)]^{1/2} \\ g_{22} &= [f(c_2) - g(c_2)]^{1/2} \end{aligned}\right\} \tag{1b}$$

$$f(c_1) = \frac{1}{(1-\frac{c^2}{c_1^2}\sin^2\theta)^{1/2}} \quad ; \quad g(c_1) = \frac{\cos\theta}{(1-\frac{c^2}{c_1^2}\sin^2\theta)^{1/2}} \tag{1c}$$

$$f(c_2) = \frac{1}{(1-\frac{c^2}{c_2^2}\sin^2\theta)^{1/2}} \quad ; \quad g(c_2) = \frac{\cos\theta}{(1-\frac{c^2}{c_2^2}\sin^2\theta)^{1/2}}$$

$$B_I(c) = \frac{1+S_2^2}{4S_1S_2-(1+S_2^2)^2} \tag{1d}$$

$$S_1^2 = 1-\frac{c^2}{c_1^2} \quad ; \quad S_2^2 = 1-\frac{c^2}{c_2^2} \tag{1e}$$

The critical radial distance was postulated to be a unique material property which was found to be $r_c = 1.3$ mm for Homalite-100 in Reference [23]. Furthermore, by setting $\theta = 0$ we obtain a chracteristic distance of

$$r_o = \frac{1}{128\pi}\left[\frac{K_I}{\sigma_{ox}} \quad V_o(c,c_1,c_2)\right]^2 \tag{2a}$$

where

$$V_o(c,c_1,c_2) = B_1(c)\{-(1+s_2^2)(2-3s_1^2)$$

$$-\frac{4s_1s_2}{1+s_2^2}(14+3s_2^2)-16s_1(s_1-s_2)+16(1+s_1^2)\} \tag{2b}$$

and the curving angle θ_c, for a stationary crack from Equation (1a) reduces to

$$\theta_c = \cos^{-1}\left[\frac{1 \pm \sqrt{1 + \frac{1024\pi}{9} r_o\left(\frac{\sigma_{ox}}{K_I}\right)^2}}{\frac{512\pi}{9} r_o\left(\frac{\sigma_{ox}}{K_I}\right)}\right] \qquad (3)$$

and c, c_1 and c_2 are the crack velocity, dilatational and distortional wave velocities, respectively. It can be easily shown that for zero crack velocity or c = 0, Equation (2) reduces to Streit and Finnie's [25] characteristic radial distance of $r_o = \frac{9}{128\pi}\left[\frac{K_I}{\sigma_{ox}}\right]^2$ for crack kinking of an initially stationary crack. This crack kinking criterion can also be used to estimate the crack branching angle for quasi-static crack branching under stress corrosion cracking conditions, provided a static counterpart of the necessary crack branching stress intensity factor can be established. The dynamic characteristic distance r_o is always less than the corresponding static r_o for crack velocities of $0 < c/c_1 \leq 0.33$ and is insensitive to the sign of σ_{ox}.

The crack kinking criterion thus states that the crack will kink at an angle of θ_c when a r_o associated with the propagating crack tip reaches a critical material property of r_c. When applied to crack branching, this crack kinking angle is one half of the included crack branching angle since the high crack branching stress intensity will result in sufficient energy release rate to create two kinked cracks simultaneously.

To recapitulate, then, crack branching will occur when the dynamic stress intensity factor reaches K_{Ib} and the crack will branch at an angle of θ_c. In the following, this crack branching criterion will be tested by re-evaluating previous dynamic experiments in which crack branching was observed. Results of eleven dynamic photoelastic results involving SEN and wedge-loaded rectangular DCB (WL-RDCB) fracture specimens are reported in the following.

CRACK BRANCHING IN HOMALITE-100 FRACTURE SPECIMENS

1. Homalite-100 SEN Specimens

The SEN specimens considered are of 3.2 mm and 9.5 mm thick Homalite-100 plates with 254 x 254 mm test section loaded in fixed grip configuration. The prescribed boundary conditions included both uniform and linearly decreasing displacements along the fixed gripped edges of the specimen. At fracture load, the crack propagated from the SEN starter crack which was saw cut and chiseled. Further details of the test setup and the test conditions can be found in Reference [26]. Figure 1 shows three frames out of a 16-frame dynamic photoelastic record of a crack propagating and branching in a 3.2 mm thick, 254 x 254 mm Homalite-100 plate loaded under fixed grip linearly varying tension.

Figure 2 shows the dynamic K_I and K_{II} variations obtained from the dynamic photoelastic patterns preceding and after crack branching of Figure 1. By extrapolating the dynamic K_I associated with two branch cracks, an after-branching dynamic stress intensity factor, $K_I = 1.2$ MPa$\sqrt{m}$ and $K_{II} = 0.45$ MPa$\sqrt{m}$ are obtained. The branching stress intensity factor, i.e. immediately prior to branching is estimated to be $K_{Ib} = 2.03$ MPa$\sqrt{m}$. Also

shown in Figure 2 are the variations in the r_o values as computed from Equation (2). Note that r_o reached a minimum value of r_c = 1.2 mm at crack branching.

Figure 3 shows another set of K_I, K_{II} and r_o for two branch cracks in a similar dynamic photoelastic experiment. By extrapolating the K_I associated with the two branch cracks, an after-branching K_I = 1.2 MPa$\sqrt{m}$ and K_{II} = -0.1 MPa$\sqrt{m}$ are obtained. Immediately prior to branching, the instantaneous dynamic stress intensity factor reached its maximum value of 2.0 MPa$\sqrt{m}$ and is consistent with the previous results. The estimated minimum r_o at crack branching was r_c = 1.3 mm. Evaluations of four other SEN tests yielded the branching stress intensity factors of K_I = 2.00 and 2.09 MPa$\sqrt{m}$, as shown in Table 1. The r_c values ranged from 1.2 to 1.4 mm.

The crack velocities in the above six tests were essentially constant at about 15 $\pm$ 5 percent of the dilitational wave velocity, c_1 = 2400 mps. Nevertheless, the crack velocity prior to and after crack branching was very close to the maximum velocity observed in all dynamic fracture tests involving Homalite-100. This so-called terminal velocity varied from test to test in a range of 0.15 to 0.20 c_1 where the crack always accelerated slightly just prior to crack branching.

The variations in the characteristic distance, r_o, which was computed from the Equation (2), for the branching cracks in the six tests all reached a minimum value prior to and at crack branching. This minimum value, which was obtained by interpolation at crack branching, was an average of 1.3 mm and is consistent with the previously measured r_c values for crack curving [23], and is further evidence that r_c is a material property. Since minimum r_o or r_c is derived through σ_{ox}, this r_c value indicates that σ_{ox} has a significant effect on crack branching.

Table 1 also shows the measured and calculated crack branching angles in the six tests. The crack branching angles, which were computed by Equation (1), for a known r_c, K_I and σ_{ox} are within 10 percent of the measured values, thus validating the use of this crack kinking criterion.

As an interesting sideline, Figure 4 shows the enlarged view of Test No. B5 where an isochromatic pattern of a pure mode II crack tip deformation, i.e. nearly pure shear state of stress, is generated around branched cracks. The mode II stress intensity factor K_{II} and remote stress σ_{ox} associated with these isochromatics are listed in Table 2. Figure 5 shows that within the 49 micro-second interval, the propagating crack turned about 81 degrees and arrested. The mixed mode stress intensity factors prior to this severe crack kinking were $K_I = 0$, $K_{II} = 0.41$ MPa$\sqrt{m}$ and $\sigma_{ox} = 0.18$ MPa, and predicted a theoretical kinking angle of 84^o which agreed well with experimentally measured angle. After crack kinking, the crack arrested and $K_I = 0.34$ MPa$\sqrt{m}$, $K_{II} = 0.08$ MPa$\sqrt{m}$ and $\sigma_{ox} = 1.4$ MPa. These results show that the crack kinking can also occur under the high K_{II} state of stress.

2. Homalite-100 WL-RDCB Specimen

As mentioned previously, the proposed crack branching criterion should be applicable to quasi-static crack branching where inertia effects in the pre-branched crack are negligible or nonexistent. Experimental data of the former were found in Homalite-100 WL-RDCB specimens where the crack immediately branched after initiating at a blunt starter crack tip. The necessary condition for branching is satisfied by the high K_{IQ}* due to the blunt

* K_{IQ} is the crack initiation stress intensity factor which is larger than the fracture toughness, K_{IC}.

crack tip. The crack branching angle, as shown by Equation (3) is a function of σ_{ox}/K_{IQ} and is thus a function of the specimen geometry.

The WL-RDCB fractured specimens considered is 76 x 152 x 9.5 mm thick of the geometry shown in Figure 6. The crack immediately branched and propagated from a single, edge-notched starter crack of length of 24.3 mm to 29.30 mm with a crack tip blunted by drilled hole of diameter of 2.2 mm to 5.0 mm. The branched crack paths of six fractured specimens are also shown in Figure 6.

In all six tests of the WL-RDCB specimens, the crack branched at initiation forming two or three branches. Table 3 summarizes the experimental test specimen information along with the measured branching angle in six WL-RDCB specimens. The angles of deviation of the post branched cracks were measured along the crack path by averaging the measured crack curving angle on front and back surfaces of the fractured specimen. Included angles for all major branches averaged 53.4 degrees, and is twice the branching angle in a SEN specimen. This averaged branch angle agrees with the experimental results of Nakasa and Takei [26] where bending of the SEN specimens due to cantilever loading resulted in a positive σ_{ox} which in turn caused larger branching angles.

Although reliable data on the crack initiation condition was lacking for this series of experiments, the crack branching angle can be estimated from standard finite element analysis. Equation (3) shows θ_c involves only the ratio of σ_{ox}/K_{IQ} and the predetermined r_c, and thus the exact applied loading condition need not be known for estimating the branch angle of an initially stationary crack. In other words, the crack branching angle in this WL-RDCB specimen is governed by the specimen geometry only provided sufficient driving force is provided to branch the crack upon initiation.

However, for a running crack, the dynamic crack branching angle, θ_c, involves not only σ_{ox}/K_I, r_o but also the crack velocity as given in Equation (1). With a unit vertical wedge loading displacement applied to the specimen, K_I and σ_{ox} were calculated by least square fitting the following plane stress crack tip displacement field of three to four sets of nodal displacements on the crack surface.

$$u_x = \frac{\sigma_{ox}}{2G} r\left(\frac{1}{1+\nu}\right) \tag{4a}$$

$$u_y = \frac{1}{G} \frac{K_I}{\sqrt{2\pi}} \sqrt{r}\left(\frac{2}{1+\nu}\right) \tag{4b}$$

G and ν in Equation (4) are shear modulus and Poisson's ratio, respectively. An average $K_{IQ}/\sigma_{ox} = 0.223\ (\sqrt{m})$ was obtained from the finite element analysis using Equation (4) and a half branch angle of $\theta_c = 26^o$ was obtained using Equation (3). This value is in good agreement with the averaged branch angle of 54 degrees shown in Table 3. Figure 7 shows two frames out of 16-frame dynamic photoelastic record of a branched cracks in a WL-RDCB specimen of 9.5 mm thick, Homalite-100 plate. Experimental details of this series of tests can be found in Reference [28]. Figure 8 shows the dynamic fracture parameters K_I, and σ_{ox} obtained from the dynamic photoelastic pattern of the three branched cracks shown in Figure 7. K_{II} which oscillated between $\pm$ 0.3 MPa$\sqrt{m}$ was not plotted in order to avoid cluttering of Figure 7. The decreasing stress intensity factor as well as the fluctuations in σ_{ox} (and K_{II}) along the post branching curved cracks are noted. Crack No. 2 arrested at K_I = 0.4 MPa$\sqrt{m}$. This arrest stress intensity factor is close to arrest stress intensity factor for Homalite-100 determined by Dally [29].

DISCUSSIONS

Table 1 shows that at the onset of branching, the instantaneous dynamic stress intensity factor reached an average maximum of 2.04 MPa$\sqrt{m}$ irrespective of specimen thickness and loading condition and the initial crack geometry. This branching stress intensity factor, K_{Ib}, is approximately 4.85 times the fracture toughness and is in agreement with that of Dally [29]. Figures 2 and 3 show that while the K_I hovers about K_{Ib}, crack branching will not occur prior to the precipitous drop in r_o. At the onset of branching, the characteristic r_o value reaches its average minimum, r_c = 1.3 mm for this material. These results show that K_{Ib} is a necessary condition for crack branching. The sufficiency condition involves the characteristic distance r_o, which is a function of the crack velocity, K_I and σ_{ox}. The ratio of K_I values prior to and after crack branching is an average of 2.2. Although this value is consistent with the postulate that crack branching occurs to dissipate fracture energy along two propagating cracks, it is higher than the expected $\sqrt{2}$ value.

It is also interesting to note that K_{II} = 0 prior to crack branching increases a small amount immediately after crack branching consistent with the postulated directional stability model [23]. Irrespective of the crack geometry and specimen thickness, crack branched when it reached $K_I = K_{Ib}$ and $r_o = r_c$, regardless of crack traveling length.

Of a total of 31 dynamic fracture tests involving WL-RDCB, 14 cracks curved and 6 branched at initiation. These results imply that crack branching in WL-RDCB specimens is observed only in few cases and is attributed to the fact that the crack propagates in a decreasing K_I field, a situation which does not promote crack branching beyond the initiation of crack extension.

The crack branching angles of Kobayashi [8], Kalthoff [21] and Christie [22] all converged to about 25-28 degrees. This agreement is not surprising since the loading conditions and the specimen geometries are quite similar in all three cases and resulted in negative σ_{ox} value which reduces the fracture angle.

CONCLUSIONS

1. A necessary and sufficient condition for dynamic crack branching is a crack branching stress intensity factor, K_{Ib}, accompanied by minimum characteristic distance $r_o = r_c$.
2. The crack instability model based on the above successfully predicted crack branching angles in Homalite-100 SEN and WL-RDCB specimens.

ACKNOWLEDGEMENT

The work reported here was obtained under ONR Contract No. 0014-76-C-0000 NR 064-478. The authors wish to acknowledge the support and encouragement of Dr. Y. Rajapakse, ONR during the course of this investigation.

Table 1

SUMMARY OF EXPERIMENTAL CRACK BRANCHING DATA AT THE ONSET OF BRANCHING IN A SINGLE EDGED NOTCHED SPECIMEN UNDER FIXED GRIP LOADING

Test No.	Plate Thickness h mm	Initial Crack Length a_o mm	Crack Length Branching a_b mm	c/c_1	At Branching K_{Ib} MPa$\sqrt{m}$	At Branching σ_{ox} MPa	At Branching r_c mm	At Branching K_{Ib}/K_{IC}	Meas. Branch Angle θ_c	Calc. Branch. Angle θ_c
B8	3.18	5.6	66.0	0.160	2.08	6.93	1.2	4.95	23^o	26
B9	3.18	4.3	177.0	0.160	2.03	5.55	1.3	4.83	30^o	24
W082270*	3.58	5.8	139.7	0.160	2.03	6.75	1.4	4.83	26^o	26
B7**	9.53	5.1	52.6	0.160	2.00	6.80	1.4	4.76	30^o	28
B5	9.53	13.5	19.1	0.16	2.08	7.08	1.2	4.95	30^o	28
B6	9.53	13.5	28.7	0.16	2.09	7.60	1.3	4.98	28^o	32
		Average		0.16	2.04	6.70	1.3	4.85	27.8	27.3

* Second Branching

** Crack Blunted

Table 2

K_{II} and σ_{ox} of Arrested Branch Cracks in Figure 4

(a) Inner Branch Crack

	14th Frame	15th Frame
K_{II}	0.4 MPa$\sqrt{m}$	0.44 MPa$\sqrt{m}$
σ_{ox}	0.32 MPa	-0.04 MPa

(b) Outer Branch Crack

	15th Frame	16th Frame
K_{II}	0.44 MPa$\sqrt{m}$	0.41 MPa$\sqrt{m}$
σ_{ox}	0.08 MPa	0.18 MPa

Table 3

SUMMARY OF CRACK BRANCHING ANGLE DISTRIBUTION IN A WEDGE LOADED RECTANGULAR DOUBLE CANTILEVER BEAM SPECIMEN

Test No.	Specimen Thickness h mm	Dia. of Blunt Notch ρ mm	Measured Branch Angle 1st Branching θ_c	Calculated 1st Branch Angle θ_c
L6B-120573	9.5	2.2	52	52
L10B-052473	9.5	2.2	52	52
L14B	9.5	5.0	55	52
L19B-013074	9.5	4.0	54	52
L27B-022474	9.5	2.4	54	52
		Average	53.4	52

References

1. Yoffe, E. H., "The Moving Griffith Crack", Phil. Mg., Vol. 42, 1951, pp. 739-750.

2. Achenbach, J. D., "Elasto Dynamic Stress Intensity Factors for a Bifurcated Crack", Prospects of Fracture Mechanics, edited by Sih et al., Noordhoff Int., 1974, pp. 319-336.

3. Achenbach, J. D., "Kinking of a Crack Under Dynamic Loading Conditions", J. Elasticity, Vol. , No. 9, 1979, pp. 113-129.

4. Anthony, S. R., and Congleton, J., "Crack Branching in Metals", Met. Sci., No. 2, 1968, pp. 158-160.

5. Congleton, J., "Practical Application of Crack Branching Measurements", Dynamic Crack Propagation, edited by G. C. Sih, Noordhoff Publ., 1973, pp. 427-438.

6. Irwin, G. R., "Comments on Dynamic Fracturing", ASTM STP 627, 1977, pp. 7-18.

7. Rossmanith, H. P., "Crack Branching in Brittle Materials, Part I", University of Maryland, Photomechanics Laboratory Report, 1977-1980.

8. Kobayashi, A. S., Wade, B. G., Bradley, W. B., and Chiu, S. T., "Crack Branching in Fracturing Homalite-100 Plates", Eng. Fract. Mech., Vol. 6, No. 1, 1974, pp. 81-92.

9. Irwin, G. R., Dally, J. W., Kobayashi, T., Fourney, W. L., Etheridge, M. J. and Rossmanith, H. P., "On the Determination of the a-K Relationships for Birefringent Polymers", Exp. Mech., Vol. 19, No. 4, 1979, pp. 121-128.

10. Kobayashi, A. S., and Ramulu, M., "Dynamic Stress Intensity Factors for Unsymmetric Dynamic Isochromatics", Exp. Mech., Vol. 21, No. 1, 1981, pp. 41-48.

11. Craggs, J. W., "On the Propagation of a Crack in an Elastic Brittle Material", J. Metals Phy. Solids, Vol. 8, 1960, pp. 66-75.

12. Döll, W., "Investigation of a Crack Branching Energy", Int. J. Fract., Vol. 11, 1975, pp. 184-186.

13. Hahn, G. T., Hoagland, R. G., and Rosenfield, A. R., "Crack Branching in A 533B Steel", Fracture 1977, Vol. 2, University of Waterloo Press, 1977, pp. 1333-1338.

14. Kobayashi, T., and Dally, J. W., "The Relation Between Crack Velocity and Stress Intensity Factor in Birefringent Polymers", ASTM STP 627, 1977, pp. 257-273.

15. Kerkhoff, F., "Wave Fractographic Investigation of Brittle Fracture Dynamics", Dynamic Crack Propagation, ed. by G. C. Sih, Noordhoff Int. Publ., Leyden, 1973, pp. 3-35.

16. Schardin, H., "Velocity Effects in Fracture", Fracture, ed. by B. L. Avorbach et al., John Wiley, 1959, pp. 297-330.

17. Acloque, P., "High Speed Cinematographic Study of the Fracture Process in Toughened Glass", Silicate Industrials, Vol. 28, 1963, p. 323.

18. Clark, A.B.J., and Irwin, G. R., "Crack Propagation Behavior", Exp. Mech., Vol. 6, 1966, pp. 321-330.

19. Sih, G. C., "Dynamic Crack Problems: Strain Energy Density Fracture Theory", Elastodynamic Crack Problems, Vol. 4, edited by G. C. Sih, Noordhoff Int. Publishing, Leyden, 1977, pp. 17-37.

20. Kitagawa, H., Yuuki, R., and Ohira, T., "Crack Morphological Aspects in Fracture Mechanics," Eng. Fract. Mech., Vol. 7, 1975, pp. 515-529.

21. Kalthoff, J. F., "On the Propagation of Bifurcated Cracks", Dynamic Crack Propagation, edited by G. C. Sih, Noordhoff Int. Publ., 1973, pp. 449-458.

22. Christie, D. G., "An Investigation of Cracks and Stress Waves in Glass and Plastics by High Speed Photography", Trans. Inc. Glass Tech., Vol. 36, 1952, pp. 74-89.

23. Ramulu, M. and Kobayashi, A. S., "Dynamic Crack Curving - A Photoelastic Evaluation", a paper submitted to Experimental Mechanics.

24. Freund, L. B., "Dynamic Crack Propagation", Mechanics of Fracture, Vol. 19, edited by F. Erdogan, ASME, 1976, pp. 105-134.

25. Streit, R., and Finnie, I., "An Experimental Investigation of Crack Path Directional Stability", Expt. Mech., Vol. 20, No. 1, 1980, pp. 17-23.

26. Bradley, W. B., "A Photoelastic Investigation of Dynamic Brittle Fracture", Ph.D. Dissertation, University of Washington, 1969.

27. Nakasa, K., and Takei, H., "Crack Branching in Delayed Failure", Engr. Fract. Mech., Vol. 11, 1979, pp. 739-751.

28. Lee, M. H., "Dynamic Photoelastic Analysis of a Compression Double Cantilever Beam Specimen", M. Sc. Thesis, University of Washington, 1975.

29. Dally, J. W., "Dynamic Photoelastic Studies of Fracture," Expt. Mech., Vol. 19, No. 10, 1979, pp. 349-367.

cbw023

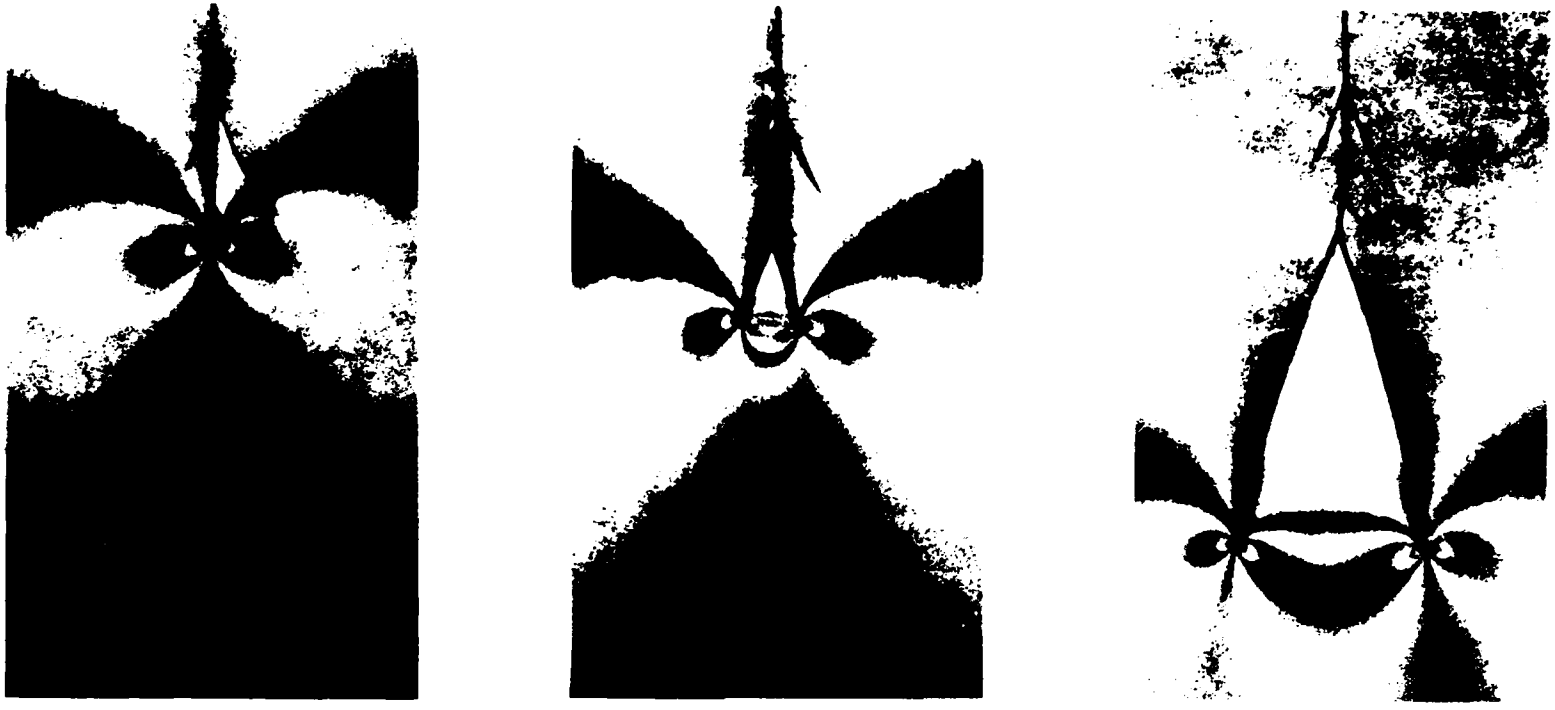

FOURTH FRAME
102 μ Seconds

FIFTH FRAME
134 μ Seconds

SEVENTH FRAME
212 μ Seconds

FIGURE 1. TYPICAL CRACK BRANCHING DYNAMIC PHOTOELASTIC PATTERNS HOMALITE 100 SINGLE EDGE NOTCHED SPECIMEN (FIXED GRIP LOADING) SPECIMEN NO. B8

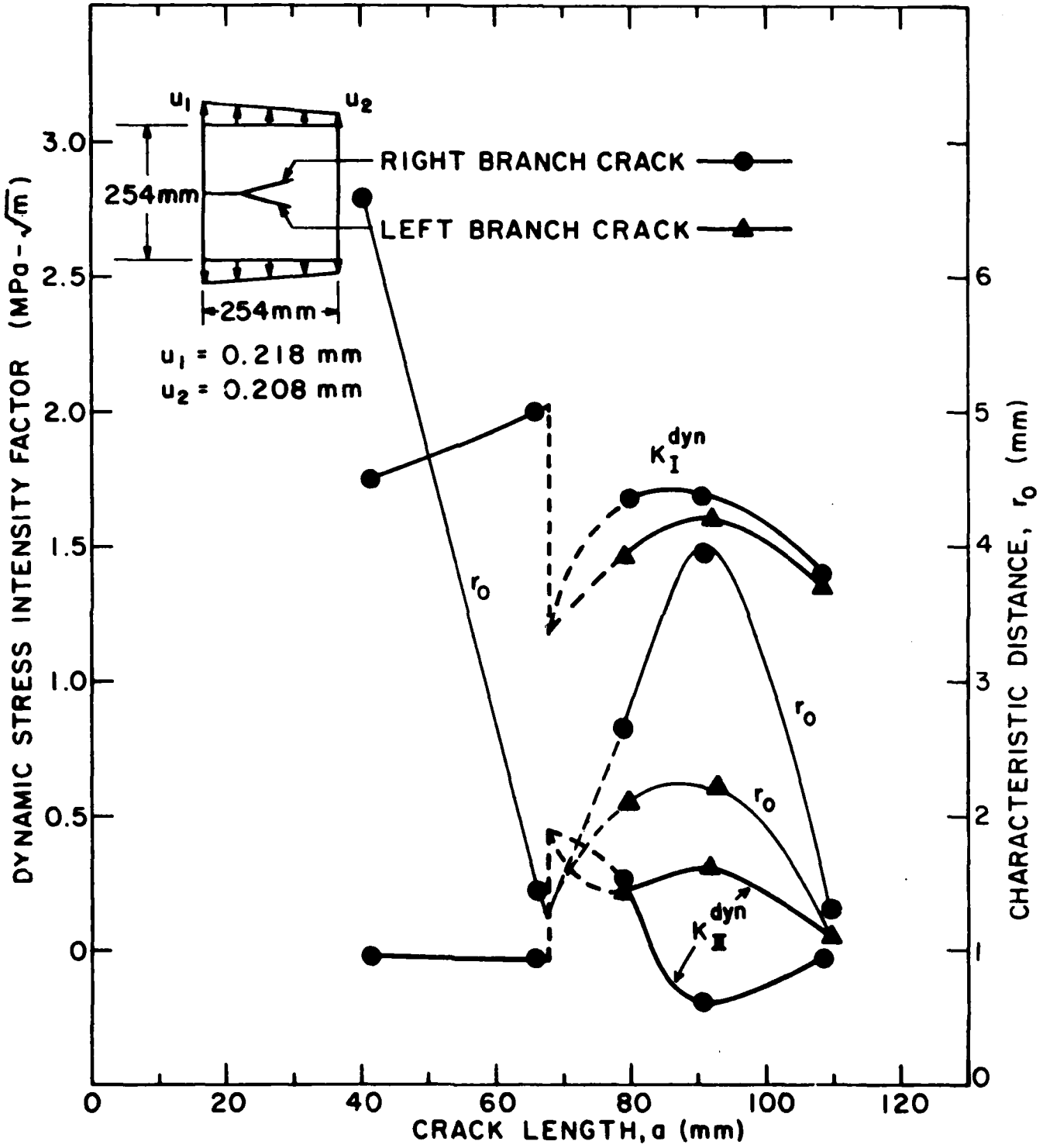

FIGURE 2. DYNAMIC STRESS INTENSITY FACTORS AND r_o OF BRANCHED CRACKS. SPECIMEN NO. B8.

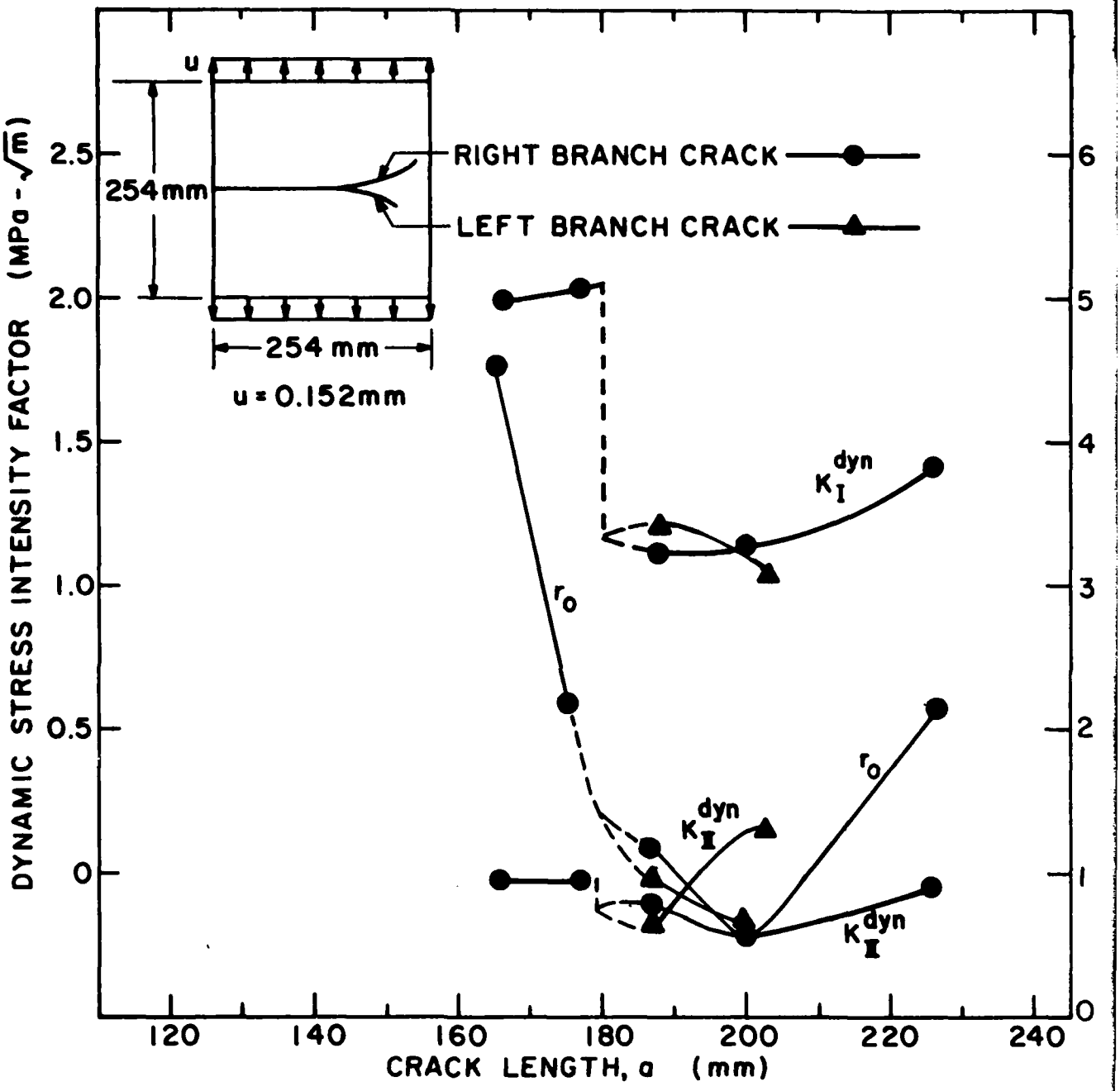

FIGURE 3. DYNAMIC STRESS INTENSITY FACTORS AND r_o OF BRANCHED CRACKS. SPECIMEN NO. B9.

FOURTEENTH FRAME
448 μ Seconds

FIFTEENTH FRAME
482 μ Seconds

(a) INNER BRANCH CRACK

FIFTEENTH FRAME
482 μ Seconds

SIXTEENTH FRAME
531 μ Seconds

(b) OUTER BRANCH CRACK

FIGURE 4. TYPICAL MODE II DYNAMIC ISOCHROMATIC PATTERNS OF ARRESTING BRANCHED CRACKS. SPECIMEN NO. B5

FIFTEENTH FRAME
482 μ Seconds

SIXTEENTH FRAME
531 μ Seconds

FIGURE 5. DYNAMIC ISOCHROMATIC PATTERNS BEFORE AND AFTER CRACK KINKING. SPECIMEN NO. B5

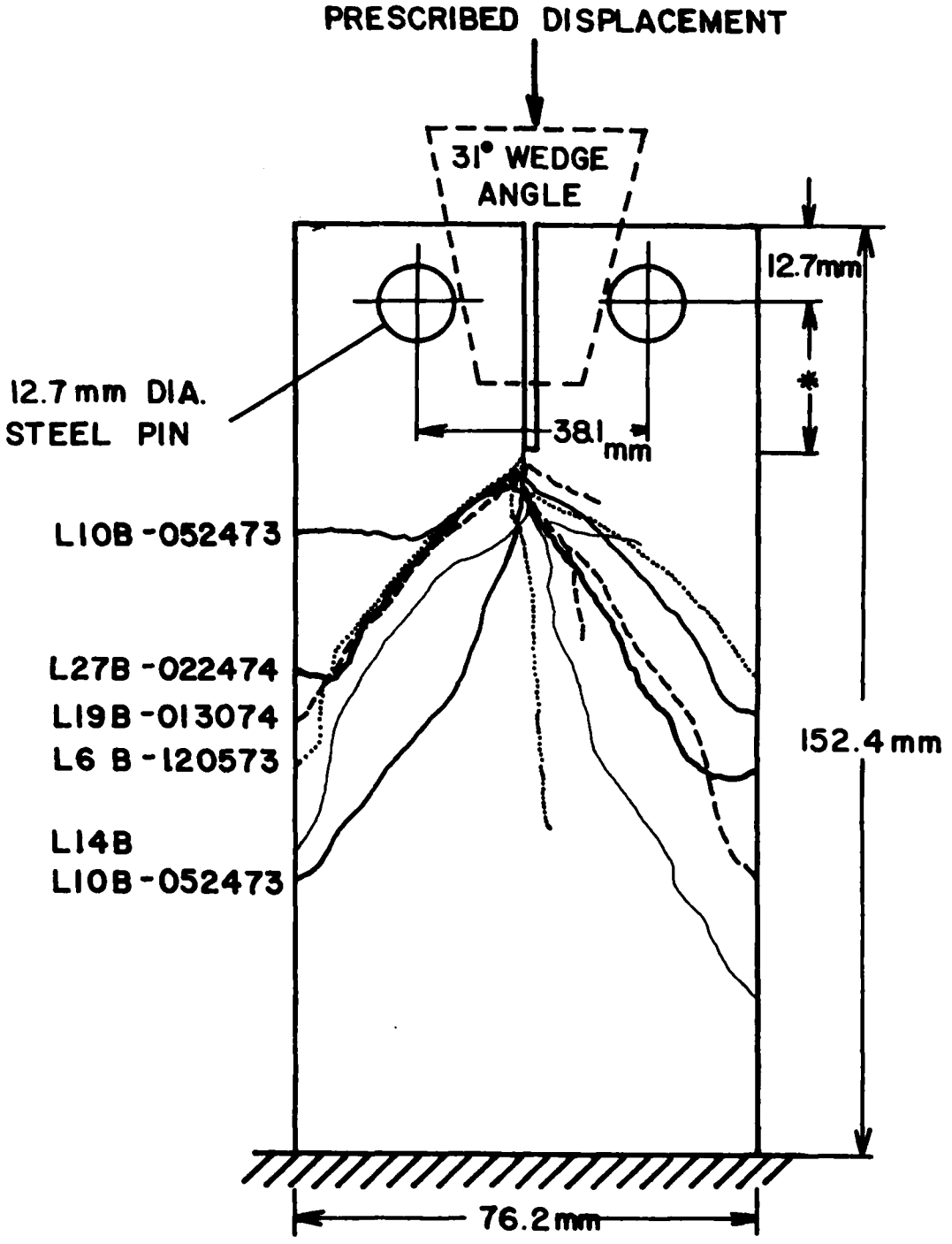

* INITIAL CRACK LENGTH

NOMINAL THICKNESS 9.5mm

FIGURE 6. BRANCHED CRACK PATHS IN WEDGE LOADED RECTANGULAR DOUBLE CANTILEVER BEAM SPECIMEN (WL-RDCB).

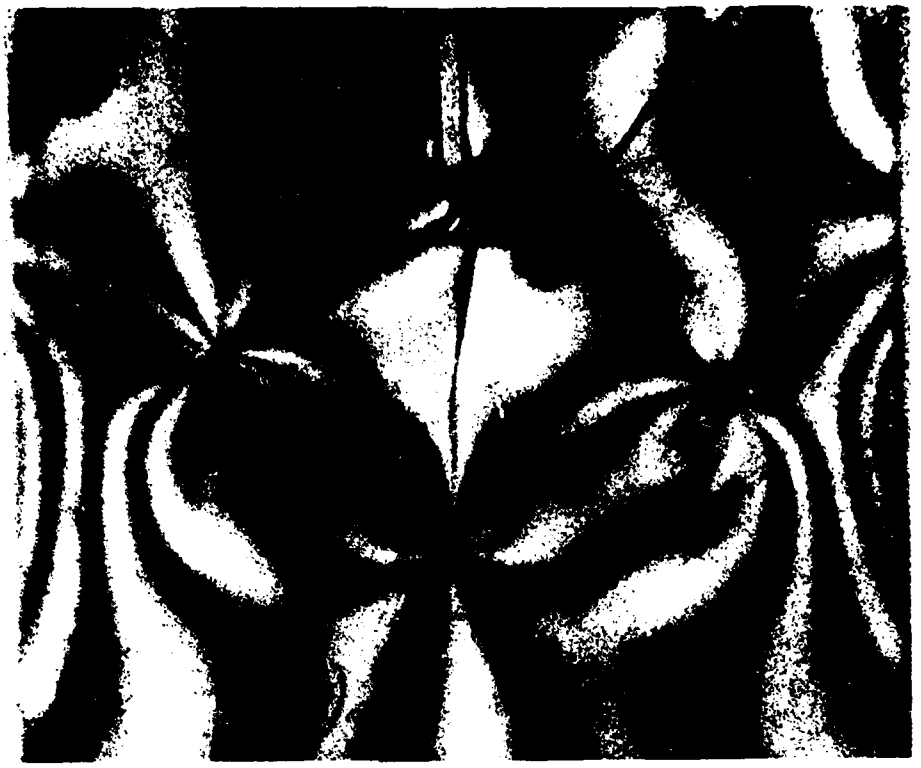

THIRD FRAME, 66 μ SECONDS

FOURTH FRAME, 84 μ SECONDS

FIGURE 7. TYPICAL PHOTOELASTIC PATTERNS OF BRANCHED CRACKS IN A WEDGE LOADED RECTANGULAR DOUBLE CANTILEVER BEAM (WL-RDCB). HOMALITE-100, SPECIMEN NO. L6B-120573.

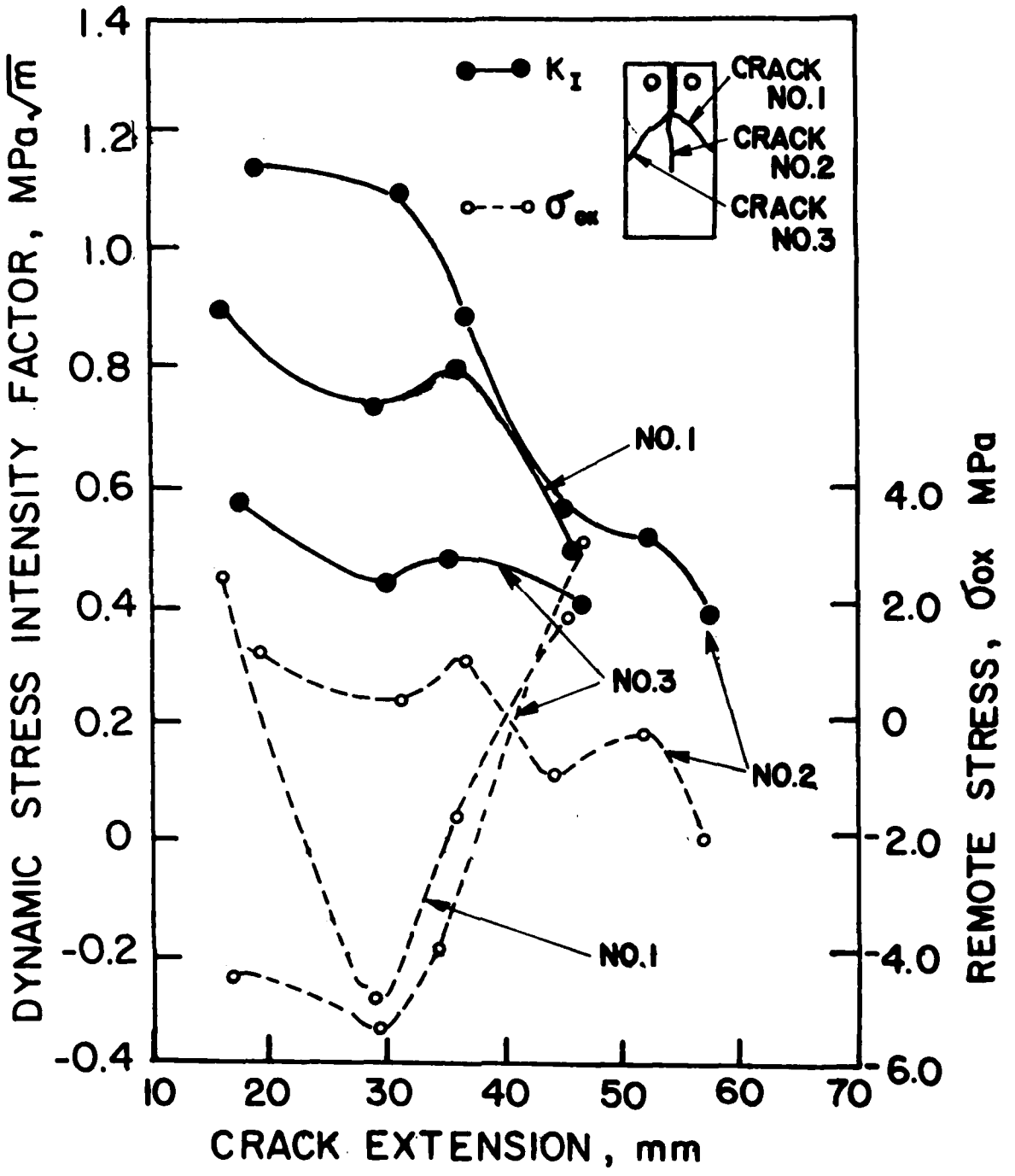

FIGURE 8 . MODE I AND II DYNAMITE STRESS INTENSITY FACTOR OF BRANCHED CRACKS SHOWN IN FIGURE 7 .

Universities (Con't.)

Professor J. Klosner
Polytechnic Institute of New York
Department of Mechanical and Aerospace Engineering
333 Jay Street
Brooklyn, New York 11201

Professor R. A. Schapery
Texas A&M University
Department of Civil Engineering
College Station, Texas 77843

Professor Walter D. Pilkey
University of Virginia
Research Laboratories for the Engineering Sciences and Applied Sciences
Charlottesville, Virginia 22901

Professor E. D. Gilimert
Clarkson College of Technology
Department of Mechanical Engineering
Potsdam, New York 13676

Dr. Walter E. Haisler
Texas A&M University
Aerospace Engineering Department
College Station, Texas 77843

Dr. Hussein A. Kamal
University of Arizona
Department of Aerospace and Mechanical Engineering
Tucson, Arizona 85721

Dr. S. J. Fenves
Carnegie-Mellon University
Department of Civil Engineering
Schenley Park
Pittsburgh, Pennsylvania 15213

Dr. Ronald L. Huston
Department of Engineering Analysis
University of Cincinnati
Cincinnati, Ohio 45221

474:MP:716:lab
78u474-619

Universities (Con't)

Professor G. C. M. Sih
Lehigh University
Institute of Fracture and Solid Mechanics
Bethlehem, Pennsylvania 18015

Professor Albert S. Kobayashi
University of Washington
Department of Mechanical Engineering
Seattle, Washington 98105

Professor Daniel Frederick
Virginia Polytechnic Institute and State University
Department of Engineering Mechanics
Blacksburg, Virginia 24061

Professor A. C. Eringen
Princeton University
Department of Aerospace and Mechanical Sciences
Princeton, New Jersey 08540

Professor E. H. Lee
Stanford University
Division of Engineering Mechanics
Stanford, California 94305

Professor Albert I. King
Wayne State University
Biomechanics Research Center
Detroit, Michigan 48202

Dr. V. R. Hodgson
Wayne State University
School of Medicine
Detroit, Michigan 48202

Dean R. A. Roley
Northwestern University
Department of Civil Engineering
Evanston, Illinois 60201

474:MP:716:lab
78u474-619

Universities (Con't)

Professor P. G. Hodge, Jr.
University of Minnesota
Department of Aerospace Engineering and Mechanics
Minneapolis, Minnesota 55455

Dr. D. C. Drucker
University of Illinois
Dean of Engineering
Urbana, Illinois 61801

Professor N. M. Newmark
University of Illinois
Department of Civil Engineering
Urbana, Illinois 61803

Professor E. Reissner
University of California, San Diego
Department of Applied Mechanics
La Jolla, California 92037

Professor William A. Nash
University of Massachusetts
Department of Mechanics and Aerospace Engineering
Amherst, Massachusetts 01002

Professor G. Herrmann
Stanford University
Department of Applied Mechanics
Stanford, California 94305

Professor J. D. Achenbach
Northwest University
Department of Civil Engineering
Evanston, Illinois 60201

Professor S. B. Dong
University of California
Department of Mechanics
Los Angeles, California 90024

Professor Burt Paul
University of Pennsylvania
Towne School of Civil and Mechanical Engineering
Philadelphia, Pennsylvania 19104

474:MP:716:lab
78u474-619

Universities (Con't)

Professor E. W. Liu
Syracuse University
Department of Chemical Engineering and Metallergy
Syracuse, New York 13210

Professor S. Bodner
Technion R&D Foundation
Haifa, Israel

Professor Werner Goldsmith
University of California
Department of Mechanical Engineering
Berkeley, California 94720

Professor R. S. Rivlin
Lehigh University
Center for the Application of Mathematics
Bethlehem, Pennsylvania 18015

Professor F. A. Cozzarelli
State University of New York at Buffalo
Division of Interdisciplinary Studies
Karr Parker Engineering Building
Chemistry Road
Buffalo, New York 14214

Professor Joseph L. Rose
Drexel University
Department of Mechanical Engineering and Mechanics
Philadelphia, Pennsylvania 19104

Professor B. E. Bonnidsen
University of Maryland
Aerospace Engineering Department
College Park, Maryland 20742

Professor Joseph A. Clark
Catholic University of America
Department of Mechanical Engineering
Washington, D.C. 20064

474:MP:716:lab
78u474-619

Universities (Con't)

Dr. Samuel B. Batdorf
University of California
School of Engineering and Applied Science
Los Angeles, California 90024

Professor Isaac Fried
Boston University
Department of Mathematics
Boston, Massachusetts 02215

Professor E. Krempl
Rensselaer Polytechnic Institute
Division of Engineering
Engineering Mechanics
Troy, New York 12181

Dr. Jack R. Vinson
University of Delaware
Department of Mechanical and Aerospace Engineering and the Center for Composite Materials
Newark, Delaware 19711

Dr. J. Duffy
Brown University
Division of Engineering
Providence, Rhode Island 02912

Dr. J. L. Swedlow
Carnegie-Mellon University
Department of Mechanical Engineering
Pittsburgh, Pennsylvania 15213

Dr. V. K. Varadan
Ohio State University Research Foundation
Department of Engineering Mechanics
Columbus, Ohio 43210

Dr. E. Shahin
University of Pennsylvania
Department of Metallurgy and Materials Science
College of Engineering and Applied Science
Philadelphia, Pennsylvania 19104

474:MP:716:lab
78u474-619

Universities (Con't)

Dr. Jackson C. S. Yang
University of Maryland
Department of Mechanical Engineering
College Park, Maryland 20742

Professor T. Y. Chang
University of Akron
Department of Civil Engineering
Akron, Ohio 44325

Professor Charles W. Bert
University of Oklahoma
School of Aerospace, Mechanical, and Nuclear Engineering
Norman, Oklahoma 73019

Professor Satya N. Atluri
Georgia Institute of Technology
School of Engineering and Mechanics
Atlanta, Georgia 30332

Professor Graham F. Carey
University of Texas at Austin
Department of Aerospace Engineering and Engineering Mechanics
Austin, Texas 78712

Dr. S. S. Wang
University of Illinois
Department of Theoretical and Applied Mechanics
Urbana, Illinois 61801

Industry and Research Institutes

Dr. Herman Robbe
Kaman AviDyne
Division of Kaman Sciences Corporation
Burlington, Massachusetts 01803

Argonne National Laboratory
Library Services Department
9700 South Cass Avenue
Argonne, Illinois 60440

474:MP:716 lab
78u474-619

Industry and Research Institutes (Con't)

Dr. M. C. Junger
Cambridge Acoustical Associates
54 Rindge Avenue Extension
Cambridge, Massachusetts 02140

Dr. V. Godino
General Dynamics Corporation
Electric Boat Division
Groton, Connecticut 06340

Dr. J. E. Greenspon
J. G. Engineering Research Associates
3831 Menlo Drive
Baltimore, Maryland 21215

Newport News Shipbuilding and Dry Dock Company
Library
Newport News, Virginia 23607

Dr. W. F. Storch
McDonnell Douglas Corporation
5301 Bolsa Avenue
Huntington Beach, California 92647

Dr. H. N. Abramson
Southwest Research Institute
8500 Culebra Road
San Antonio, Texas 78284

Dr. R. C. DeHart
Southwest Research Institute
8500 Culebra Road
San Antonio, Texas 78284

Dr. N. L. Baron
Weidlinger Associates
110 East 59th Street
New York, New York 10022

Dr. T. L. Geers
Lockheed Missiles and Space Company
3251 Hanover Street
Palo Alto, California 94304

Mr. William Caywood
Applied Physics Laboratory
Johns Hopkins Road
Laurel, Maryland 20810

Industry and Research Institutes (Con't)

Dr. Robert E. Dunham
Pacifica Technology
P.O. Box 148
Del Mar, California 92014

Dr. M. F. Kaminski
Battelle Columbus Laboratories
505 King Avenue
Columbus, Ohio 43201

Dr. A. A. Hochrein
Dandelion Associates, Inc.
Springlake Research Road
15110 Frederick Road
Woodbine, Maryland 21797

Dr. James M. Jones
Swanson Service Corporation
P.O. Box 3613
Huntington Beach, California 92646

Dr. Robert E. Nickell
Applied Science and Technology
3344 North Torrey Pines Court
Suite 220
La Jolla, California 92037

Dr. Kevin Thomas
Westinghouse Electric Corp.
Advanced Reactors Division
P. O. Box 158
Madison, Pennsylvania 15663

Part 1 - Government
Administrative and Liaison Activities

Office of Naval Research
Department of the Navy
Arlington, Virginia 22217
Attn: Code 474 (2)
Code 471
Code 200

Director
Office of Naval Research
Branch Office
666 Summer Street
Boston, Massachusetts 02210

Director
Office of Naval Research
Branch Office
536 South Clark Street
Chicago, Illinois 60605

Director
Office of Naval Research
Branch Office
1030 East Green Street
Pasadena, California 91106

Naval Research Laboratory (6)
Code 2627
Washington, D.C. 20375

Defense Documentation Center (12)
Cameron Station
Alexandria, Virginia 22314

Navy

Undersea Explosion Research Division
Naval Ship Research and Development
Center
Norfolk Naval Shipyard
Portsmouth, Virginia 23709
Attn: Dr. E. Palmer, Code 177

Navy (Con't.)

Naval Research Laboratory
Washington, D.C. 20375
Attn: Code 8400
8410
8430
8440
6300
6390
6380

David W. Taylor Naval Ship Research
and Development Center
Annapolis, Maryland 21402
Attn: Code 2740
28
281

Naval Weapons Center
China Lake, California 93555
Attn: Code 4062
4520

Commanding Officer
Naval Civil Engineering Laboratory
Code L31
Port Hueneme, California 93041

Naval Surface Weapons Center
White Oak
Silver Spring, Maryland 20910
Attn: Code R-10
G-402
K-82

Technical Director
Naval Ocean Systems Center
San Diego, California 92152

Supervisor of Shipbuilding
U.S. Navy
Newport News, Virginia 23607

Navy Underwater Sound
Reference Division
Naval Research Laboratory
P.O. Box 8337
Orlando, Florida 32806

474:HF:716:lab
78u474-619

Navy (Con't.)

Chief of Naval Operations
Department of the Navy
Washington, D.C. 20350
Attn: Code OP-098

Strategic Systems Project Office
Department of the Navy
Washington, D.C. 20376
Attn: SSP-200

Naval Air Systems Command
Department of the Navy
Washington, D.C. 20361
Attn: Code 5302 (Aerospace and Structures)
604 (Technical Library)
320R (Structures)

Naval Air Development Center
Warminster, Pennsylvania 18974
Attn: Aerospace Mechanics
Code 606

U.S. Naval Academy
Engineering Department
Annapolis, Maryland 21402

Naval Facilities Engineering Command
200 Stovall Street
Alexandria, Virginia 22332
Attn: Code 03 (Research and Development)
04B
045
14114 (Technical Library)

Naval Sea Systems Command
Department of the Navy
Washington, D.C. 20362
Attn: Code 05H
312
322
323
05R
32R

Navy (Con't.)

Commander and Director
David W. Taylor Naval Ship
Research and Development Center
Bethesda, Maryland 20084
Attn: Code 042
17
172
173
174
1800
1844
012.2
1900
1901
1945
1960
1962

Naval Underwater Systems Center
Newport, Rhode Island 02840
Attn: Dr. R. Trainor

Naval Surface Weapons Center
Dahlgren Laboratory
Dahlgren, Virginia 22448
Attn: Code G04
G20

Technical Director
Mare Island Naval Shipyard
Vallejo, California 94592

U.S. Naval Postgraduate School
Library
Code 0384
Monterey, California 93940

Webb Institute of Naval Architecture
Attn: Librarian
Crescent Beach Road, Glen Cove
Long Island, New York 11542

Army

Commanding Officer (2)
U.S. Army Research Office
P.O. Box 12211
Research Triangle Park, NC 27709
Attn: Mr. J. J. Murray, CRD-AA-IP

474:HF:716:lab
78u474-619

Army (Con't.)

Watervliet Arsenal
MAGGS Research Center
Watervliet, New York 12189
Attn: Director of Research

U.S. Army Materials and Mechanics
Research Center
Watertown, Massachusetts 02172
Attn: Dr. R. Shea, SMUMR-T

U.S. Army Missile Research and
Development Center
Redstone Scientific Information
Center
Chief, Document Section
Redstone Arsenal, Alabama 35809

Army Research and Development
Center
Fort Belvoir, Virginia 22060

NASA

National Aeronautics and Space
Administration
Structures Research Division
Langley Research Center
Langley Station
Hampton, Virginia 23365

National Aeronautics and Space
Administration
Associate Administrator for Advanced
Research and Technology
Washington, D.C. 20546

Air Force

Wright-Patterson Air Force Base
Dayton, Ohio 45433
Attn: AFFDL (FB)
(FBR)
(FBE)
(FBS)
AFML (MBM)

Air Force (Con't.)

Chief Applied Mechanics Group
U.S. Air Force Institute of Technology
Wright-Patterson Air Force Base
Dayton, Ohio 45433

Chief, Civil Engineering Branch
WLRC, Research Division
Air Force Weapons Laboratory
Kirtland Air Force Base
Albuquerque, New Mexico 87117

Air Force Office of Scientific Research
Bolling Air Force Base
Washington, D.C. 20332
Attn: Mechanics Division

Department of the Air Force
Air University Library
Maxwell Air Force Base
Montgomery, Alabama 36112

Other Government Activities

Commandant
Chief, Testing and Development Division
U.S. Coast Guard
1300 E Street, NW.
Washington, D.C. 20226

Technical Director
Marine Corps Development
and Education Command
Quantico, Virginia 22134

Director Defense Research
and Engineering
Technical Library
Room 3C128
The Pentagon
Washington, D.C. 20301

474:HF:716:lab
78u474-619

Other Government Activities (Con't)

Dr. M. Gaus
National Science Foundation
Environmental Research Division
Washington, D.C. 20550

Library of Congress
Science and Technology Division
Washington, D.C. 20540

Director
Defense Nuclear Agency
Washington, D.C. 20305
Attn: SPSS

Mr. Jerome Persh
Staff Specialist for Materials
and Structures
OUSDR&E, The Pentagon
Room 3D1089
Washington, D.C. 20301

Chief, Airframe and Equipment Branch
FS-120
Office of Flight Standards
Federal Aviation Agency
Washington, D.C. 20553

National Academy of Sciences
National Research Council
Ship Hull Research Committee
2101 Constitution Avenue
Washington, D.C. 20418
Attn: Mr. A. R. Lytle

National Science Foundation
Engineering Mechanics Section
Division of Engineering
Washington, D.C. 20550

Picatinny Arsenal
Plastics Technical Evaluation Center
Attn: Technical Information Section
Dover, New Jersey 07801

Maritime Administration
Office of Maritime Technology
14th and Constitution Avenue, NW.
Washington, D.C. 20230

474:HF:716:lab
78u474-619

PART 2 - Contractors and Other Technical Collaborators

Universities

Dr. J. Tinsley Oden
University of Texas at Austin
345 Engineering Science Building
Austin, Texas 78712

Professor Julius Miklowitz
California Institute of Technology
Division of Engineering
and Applied Sciences
Pasadena, California 91109

Dr. Harold Liebowitz, Dean
School of Engineering and
Applied Science
George Washington University
Washington, D.C. 20052

Professor Eli Sternberg
California Institute of Technology
Division of Engineering and
Applied Sciences
Pasadena, California 91109

Professor Paul M. Naghdi
University of California
Department of Mechanical Engineering
Berkeley, California 94720

Professor A. J. Durelli
Oakland University
School of Engineering
Rochester, Missouri 48063

Professor F. L. DiMaggio
Columbia University
Department of Civil Engineering
New York, New York 10027

Professor Norman Jones
The University of Liverpool
Department of Mechanical Engineering
P. O. Box 147
Brownlow Hill
Liverpool L69 3BX
England

Professor E. J. Skudrzyk
Pennsylvania State University
Applied Research Laboratory
Department of Physics
State College, Pennsylvania 16801

Universities (Con't.)

Professor J. Kleemar
Polytechnic Institute of New York
Department of Mechanical and
Aerospace Engineering
333 Jay Street
Brooklyn, New York 11201

Professor R. A. Schapery
Texas A&M University
Department of Civil Engineering
College Station, Texas 77843

Professor Walter D. Pilkey
University of Virginia
Research Laboratories for the
Engineering Sciences and
Applied Sciences
Charlottesville, Virginia 22901

Professor K. D. Willmert
Clarkson College of Technology
Department of Mechanical Engineering
Potsdam, New York 13676

Dr. Walter E. Haisler
Texas A&M University
Aerospace Engineering Department
College Station, Texas 77843

Dr. Hussein A. Kamal
University of Arizona
Department of Aerospace and
Mechanical Engineering
Tucson, Arizona 85721

Dr. S. J. Fenves
Carnegie-Mellon University
Department of Civil Engineering
Schenley Park
Pittsburgh, Pennsylvania 15213

Dr. Ronald L. Huston
Department of Engineering Analysis
University of Cincinnati
Cincinnati, Ohio 45221

Universities (Con't)

Professor G. C. M. Sih
Lehigh University
Institute of Fracture and
Solid Mechanics
Bethlehem, Pennsylvania 18015

Professor Albert S. Kobayashi
University of Washington
Department of Mechanical Engineering
Seattle, Washington 98105

Professor Daniel Frederick
Virginia Polytechnic Institute and
State University
Department of Engineering Mechanics
Blacksburg, Virginia 24061

Professor A. C. Eringen
Princeton University
Department of Aerospace and
Mechanical Sciences
Princeton, New Jersey 08540

Professor E. H. Lee
Stanford University
Division of Engineering Mechanics
Stanford, California 94305

Professor Albert I. King
Wayne State University
Biomechanics Research Center
Detroit, Michigan 48202

Dr. V. R. Hodgson
Wayne State University
School of Medicine
Detroit, Michigan 48202

Dean B. A. Boley
Northwestern University
Department of Civil Engineering
Evanston, Illinois 60201

Universities (Con't)

Professor P. G. Hodge, Jr.
University of Minnesota
Department of Aerospace Engineering
and Mechanics
Minneapolis, Minnesota 55455

Dr. D. C. Drucker
University of Illinois
Dean of Engineering
Urbana, Illinois 61801

Professor N. M. Newmark
University of Illinois
Department of Civil Engineering
Urbana, Illinois 61803

Professor E. Reissner
University of California, San Diego
Department of Applied Mechanics
La Jolla, California 92037

Professor William A. Nash
University of Massachusetts
Department of Mechanics and
Aerospace Engineering
Amherst, Massachusetts 01002

Professor G. Herrmann
Stanford University
Department of Applied Mechanics
Stanford, California 94305

Professor J. D. Achenbach
Northwest University
Department of Civil Engineering
Evanston, Illinois 60201

Professor S. B. Dong
University of California
Department of Mechanics
Los Angeles, California 90024

Professor Burt Paul
University of Pennsylvania
Towne School of Civil and
Mechanical Engineering
Philadelphia, Pennsylvania 19104

Universities (Con't)

Professor H. W. Liu
Syracuse University
Department of Chemical Engineering
and Metallurgy
Syracuse, New York 13210

Professor S. Bodner
Technion R&D Foundation
Haifa, Israel

Professor Werner Goldsmith
University of California
Department of Mechanical Engineering
Berkeley, California 94720

Professor R. S. Rivlin
Lehigh University
Center for the Application
of Mathematics
Bethlehem, Pennsylvania 18015

Professor F. A. Cozzarelli
State University of New York at
Buffalo
Division of Interdisciplinary Studies
Karr Parker Engineering Building
Chemistry Road
Buffalo, New York 14214

Professor Joseph L. Rose
Drexel University
Department of Mechanical Engineering
and Mechanics
Philadelphia, Pennsylvania 19104

Professor B. K. Donaldson
University of Maryland
Aerospace Engineering Department
College Park, Maryland 20742

Professor Joseph A. Clark
Catholic University of America
Department of Mechanical Engineering
Washington, D.C. 20064

Universities (Con't)

Dr. Samuel S. Batdorf
University of California
School of Engineering
and Applied Science
Los Angeles, California 90024

Professor Isaac Fried
Boston University
Department of Mathematics
Boston, Massachusetts 02215

Professor E. Krempl
Rensselaer Polytechnic Institute
Division of Engineering
Engineering Mechanics
Troy, New York 12181

Dr. Josh E. Vinson
University of Delaware
Department of Mechanical and Aerospace
Engineering and the Center for
Composite Materials
Newark, Delaware 19711

Dr. J. Duffy
Brown University
Division of Engineering
Providence, Rhode Island 02912

Dr. J. L. Swedlow
Carnegie-Mellon University
Department of Mechanical Engineering
Pittsburgh, Pennsylvania 15213

Dr. V. K. Varadan
Ohio State University Research Foundation
Department of Engineering Mechanics
Columbus, Ohio 43210

Dr. S. Rhodin
University of Pennsylvania
Department of Metallurgy and
Materials Science
College of Engineering and
Applied Science
Philadelphia, Pennsylvania 19104

Universities (Con't)

Dr. Jackson C. S. Yang
University of Maryland
Department of Mechanical Engineering
College Park, Maryland 20742

Professor T. Y. Chang
University of Akron
Department of Civil Engineering
Akron, Ohio 44325

Professor Charles W. Bert
University of Oklahoma
School of Aerospace, Mechanical,
and Nuclear Engineering
Norman, Oklahoma 73019

Professor Satya N. Atluri
Georgia Institute of Technology
School of Engineering and
Mechanics
Atlanta, Georgia 30332

Professor Graham F. Carey
University of Texas at Austin
Department of Aerospace Engineering
and Engineering Mechanics
Austin, Texas 78712

Dr. S. S. Wang
University of Illinois
Department of Theoretical and
Applied Mechanics
Urbana, Illinois 61801

Industry and Research Institutes

Dr. Herman Robbs
Kaman AviDyne
Division of Kaman
Sciences Corporation
Burlington, Massachusetts 01803

Argonne National Laboratory
Library Services Department
9700 South Cass Avenue
Argonne, Illinois 60440

Industry and Research Institutes (Con't)

Dr. M. C. Junger
Cambridge Acoustical Associates
54 Rindge Avenue Extension
Cambridge, Massachusetts 02140

Dr. V. Godino
General Dynamics Corporation
Electric Boat Division
Groton, Connecticut 06340

Dr. J. E. Greenspon
J. G. Engineering Research Associates
3831 Hamlo Drive
Baltimore, Maryland 21215

Newport News Shipbuilding and
Dry Dock Company
Library
Newport News, Virginia 23607

Dr. W. F. Bozich
McDonnell Douglas Corporation
3301 Holes Avenue
Huntington Beach, California 92647

Dr. H. N. Abramson
Southwest Research Institute
8500 Culebra Road
San Antonio, Texas 78284

Dr. B. C. DeHart
Southwest Research Institute
8500 Culebra Road
San Antonio, Texas 78284

Dr. M. L. Baron
Weidlinger Associates
110 East 59th Street
New York, New York 10022

Dr. T. L. Geers
Lockheed Missiles and Space Company
3251 Hanover Street
Palo Alto, California 94304

Mr. William Caywood
Applied Physics Laboratory
Johns Hopkins Road
Laurel, Maryland 20810

Industry and Research Institutes (Con't)

Dr. Robert E. Dunham
Pacifica Technology
P.O. Box 148
Del Mar, California 92014

Dr. M. P. Kamminen
Battelle Columbus Laboratories
505 King Avenue
Columbus, Ohio 43201

Dr. A. A. Hochrein
Dandelion Associates, Inc.
Springlake Research Road
15110 Frederick Road
Woodbine, Maryland 21797

Dr. James W. Jones
Swanson Service Corporation
P.O. Box 3415
Huntington Beach, California 92646

Dr. Robert E. Nickell
Applied Science and Technology
3344 North Torrey Pines Court
Suite 320
La Jolla, California 92037

Dr. Kevin Thomas
Westinghouse Electric Corp.
Advanced Reactors Division
P. O. Box 158
Madison, Pennsylvania 15663

Unclassified

SECURITY CLASSIFICATION OF THIS PAGE (When Data Entered)

REPORT DOCUMENTATION PAGE		READ INSTRUCTIONS BEFORE COMPLETING FORM
1. REPORT NUMBER UWA/DME/TR-82/43	2. GOVT ACCESSION NO. AD-A114 525	3. RECIPIENT'S CATALOG NUMBER
4. TITLE (and Subtitle) Dynamic Crack Branching - A Photoelastic Evaluation		5. TYPE OF REPORT & PERIOD COVERED Technical Report 6. PERFORMING ORG. REPORT NUMBER UWA/DME/TR-82/43
7. AUTHOR(s) M. Ramulu, A. S. Kobayashi & B. S.-J. Kang		8. CONTRACT OR GRANT NUMBER(s) N00014-76-C-0060
9. PERFORMING ORGANIZATION NAME AND ADDRESS University of Washington Dept. of Mechanical Engineering FU-10 Seattle, WA 98195		10. PROGRAM ELEMENT, PROJECT, TASK AREA & WORK UNIT NUMBERS NR 064-478
11. CONTROLLING OFFICE NAME AND ADDRESS Office of Naval Research Arlington, VA 22217		12. REPORT DATE May 1982 13. NUMBER OF PAGES 19
14. MONITORING AGENCY NAME & ADDRESS(if different from Controlling Office)		15. SECURITY CLASS. (of this report) Unclassified 15a. DECLASSIFICATION/DOWNGRADING SCHEDULE

16. DISTRIBUTION STATEMENT (of this Report)

Unlimited Distribution

17. DISTRIBUTION STATEMENT (of the abstract entered in Block 20, if different from Report)

18. SUPPLEMENTARY NOTES

19. KEY WORDS (Continue on reverse side if necessary and identify by block number)

Dynamic fracture crack branching, ~~crack curving, dy~~namic photoelasticity, finite element analysis

20. ABSTRACT (Continue on reverse side if necessary and identify by block number)

A necessary and sufficient condition for crack branching based on a crack branching stress intensity factor, K_{Ib}, accompanied by a minimum characteristic distance of r_c is proposed. This crack branching criterion is evaluated by dynamic photoelastic experiments involving crack branching of six single-edged notch specimens and six wedge-loaded rectangulr double cantilever beam specimens. Consistent crack branching at K_{Ib} = 2.04 MPa$\sqrt{m}$ and r_c = 1.3 mm verified this crack branching criterion. The crack branching angle predicted by

DD FORM 1 JAN 73 1473 EDITION OF 1 NOV 68 IS OBSOLETE
S/N 0102-014-6601

Unclassified

SECURITY CLASSIFICATION OF THIS PAGE (When Data Entered)

20. (continued)

this crack branching criterion agreed well with those measured in the crack branching experiments.

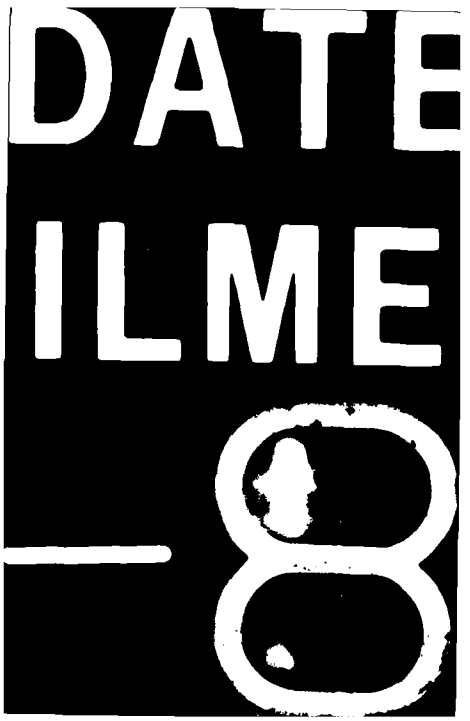
DATE
ILME
8